BIODIVERSITAS
Volume 26, Number 11, November 2025
Pages: 5703-5713

ISSN: 1412-033X
E-ISSN: 2085-4722
DOI: 10.13057/biodiv/d261129

Chloroplast genome variation and phylogeny of mutant *Typhonium flagelliforme* (Araceae) from Indonesia

NESTI FRONIKA SIANIPAR[1,2,♥], ZIDNI MUFLIKHATI[2], ENDANG RAHMAT[1], REFLINUR[3], KHOIRUNNISA ASSIDQI[1,2], DWIYANTARI WIDYANINGRUM[1]

[1]Department of Biotechnology, Faculty of Engineering, Universitas Bina Nusantara. Jl. K. H. Syahdan No. 9, Jakarta 11480, Jakarta, Indonesia. Tel.: +62-21-534-5830, ♥email: nsianipar@binus.edu
[2]Food Biotechnology Research Center, Universitas Bina Nusantara. Jl. K. H. Syahdan No. 9, Jakarta 11480, Jakarta, Indonesia
[3]Research Center for Applied Botany, Research Organization for Life Sciences and Environment, National Research and Innovation Agency (BRIN). Jl. Raya Jakarta-Bogor Km. 46, Cibinong, Bogor 16911, West Java, Indonesia

Manuscript received: 12 August 2025. Revision accepted: 6 November 2025.

Abstract. *Sianipar NF, Muflikhati Z, Rahmat E, Reflinur, Assidqi K, Widyaningrum D. 2025. Chloroplast genome variation and phylogeny of mutant* Typhonium flagelliforme *(Araceae) from Indonesia. Biodiversitas 26: 5703-5713. Typhonium flagelliforme* (rodent tuber) is an indigenous Indonesian medicinal plant valued for its anticancer properties. Mutation induced by gamma irradiation have produced mutant accessions with enhanced bioactivity, yet the underlying genetic basis remains poorly understood. To address this gap, we conducted a comparative analysis of complete chloroplast genomes from wild-type and mutant *T. flagelliforme*. Both genomes displayed a typical quadripartite structure, with lengths of 167,195 bp (wild-type) and 167,204 bp (mutant). Gene annotation revealed 118 genes in the wild-type, but only 116 in the mutant, with the absence of *psaL* and *petN*, genes related to photosystem I and the cytochrome b6f complex. In addition to both accessions preferring A/U-ending codons, simple sequence repeat (SSR) profiling identified 131 motifs in the wild type and 132 in the mutant. Divergent hotspot analysis detected high nucleotide diversity in loci, such as *ndhE* and *ccsA*. Phylogenetic reconstruction confirmed that both accessions form a monophyletic clade closely related to *T. blumei*, reinforcing their genetic proximity within the genus. These findings demonstrate that induced mutation results in localized plastome alterations without disrupting overall structural stability, thereby providing valuable genomic resources for phylogenetic inference, biodiversity conservation, and marker-assisted breeding in *Typhonium* and related Araceae taxa.

Keywords: Araceae, chloroplast genome, molecular marker, phylogeny, *Typhonium flagelliforme*

INTRODUCTION

Typhonium flagelliforme (G.Lodd.) Blume, commonly known as rodent tuber, is a medicinal plant native to Indonesia that has long been used in traditional health practices. Its pharmacological importance is mainly associated with bioactive compounds that exhibit anti-inflammatory, anticancer, and antimicrobial activities (Lai et al. 2008). Extracts from this species have been shown to induce apoptosis and inhibit tumor growth in various cell lines, which underscores its potential in the development of novel therapeutic agents (Mohan et al. 2010; Nobakht et al. 2014). Due to its ethnomedicinal relevance, *T. flagelliforme* has attracted attention not only from local communities but also from researchers focusing on phytopharmaceuticals.

Mutation breeding strategies, such as somaclonal variation and gamma irradiation have been applied to enhance the medicinal value of *T. flagelliforme* (Sianipar et al. 2013; Sianipar and Purnamaningsih 2018). These approaches have generated mutant lines with higher concentrations of secondary metabolites and stronger cytotoxic effects compared to wild-type plants (Sianipar et al. 2023). Sianipar et al. (2024) reported that induced mutations can alter metabolic pathways, leading to increase the levels of fatty acid, terpenoid, and alkaloid production in mutant accessions. Despite these promising results, the genetic mechanisms underlying such improvements remain largely unexplored. Without a molecular understanding, efforts to optimize breeding, conservation, and utilization of *T. flagelliforme* remain constrained.

Chloroplast genomes (cpDNA) provide an important entry point for investigating plant evolution, diversity, and biosynthetic potential (Yan et al. 2025). In angiosperms, cpDNA is maternally inherited and exhibits a conserved quadripartite structure comprising Large Single-Copy (LSC) and Small Single-Copy (SSC) regions flanked by two Inverted Repeats (IRs) (Wang and Lanfear 2019). While chloroplasts do not directly encode complete secondary metabolic pathways, they contribute precursors, energy, and regulatory signals essential for metabolite biosynthesis (Cackett et al. 2022). This makes cpDNA variation highly relevant to the study of medicinal plants, as structural or sequence differences may affect traits linked to bioactive compound production.

Advances in high-throughput sequencing have enabled the assembly and comparative analysis of complete cp genomes in diverse plant taxa. For instance, comparative cp genomics in members of Lamiaceae, Asteraceae, and Poaceae has revealed divergence hotspots that serve as molecular markers for phylogenetic resolution and species authentication (Zhao et al. 2021; Song et al. 2023). Within the family Araceae, cp genomes of *Colocasia gigantea*,

Caladium bicolor, and *Xanthosoma sagittifolium* have been reported, revealing structural diversity and variation in gene content (Hu et al. 2023). However, despite Indonesia's status as a center of Araceae diversity, genomic resources for many indigenous medicinal species remain scarce.

Previous studies on *T. flagelliforme* have primarily focused on its phytochemical composition and cytotoxicity properties, such as Sianipar et al. (2016, 2017, 2023, 2024) and Purnamaningsih et al. (2018), while cp genome aspects remain largely unexplored in mutant *T. flagelliforme*. Currently, only one cp genome sequence of *T. flagelliforme* is available in public databases, representing a single accession. No comparative studies have examined cp genome differences between wild-type and mutant lines, even though mutation breeding is widely applied to enhance its medicinal traits. Gamma irradiation may induce genomic changes affecting photosynthesis-related genes, codon usage, and repetitive sequences, which could influence secondary metabolism (Jeong et al. 2024). Therefore, comparative chloroplast genomics between wild-type and mutant accessions could reveal genomic variation relevant to both evolution and phytochemical potential. This study presents the first comparative analysis of complete chloroplast genomes from Indonesian wild-type and gamma-irradiated mutant T. *flagelliforme*. This study aimed to characterize plastome structure and gene content, analyze codon usage and SSR profiles, identify divergence hotspots, and infer phylogenetic relationships with related *Typhonium* species. The findings provide new genomic resources to support biodiversity conservation, molecular breeding, and phytopharmaceutical development of *T. flagelliforme* and related taxa of Araceae.

MATERIALS AND METHODS

Plant materials

Wild-type and mutant *Typhonium flagelliforme* plants were cultivated in a controlled greenhouse at Universitas Bina Nusantara, Bekasi, West Java, Indonesia, under standard horticultural conditions. Mutants were generated through somaclonal variation and gamma irradiation (Sianipar and Purnamaningsih 2018), while wild-type plants were collected from a natural population at Universitas Bina Nusantara. The mutant variety Tipobio holds Plant Variety Protection rights (No. 00489/PPVT/S/2020) with voucher specimens TYFL001.

Procedures

Chloroplast DNA extraction

Young leaves (<3 weeks old) were harvested during the dry season to minimize polysaccharide contamination, flash-frozen in liquid nitrogen, and ground into a fine powder. Total genomic DNA was extracted using the Quick-DNA Plant Kit (Zymo Research, USA) following the manufacturer's instructions. DNA quality and concentration were assessed using a NanoDrop 2000 spectrophotometer (Thermo Scientific, USA), Qubit dsDNA HS Assay Kit (Thermo Scientific, USA), and 1% agarose gel electrophoresis. DNA integrity and fragment size distribution were evaluated on the 4150 TapeStation (Agilent Technologies, USA).

Chloroplast genome sequencing

High-quality DNA (1 µg) was used for library preparation and sequenced on the PromethION platform (Oxford Nanopore Technologies, UK). Sequencing proceeded until ≥50× coverage was achieved for all regions. Base calling was performed with Dorado v0.5.1 in high-accuracy mode.

Data analysis

Sequence raw data processing

Raw reads were quality-checked using NanoPlot v1.41.0 (De Coster et al. 2018) and mapped to the *T. flagelliforme* chloroplast genome (GenBank OR583019.1) with minimap2 v2.26 (Li 2018). Mapped reads were extracted using SAMtools v1.17 (Danecek et al. 2021). De novo assembly was performed with Flye v2.9.3 (Kolmogorov et al. 2019) and polished using Medaka v1.11.0 (Oxford Nanopore Technologies). Assembly completeness was evaluated with QUAST v5.2.0 (Gurevich et al. 2013) and Qualimap v2.2.2 (Okonechnikov et al. 2016). Annotation was carried out using GeSeq (Tillich et al. 2017) and genome maps were generated with OGDRAW v1.3.1 (Greiner et al. 2019). Species identity was verified with BLASTn against the NCBI nr/nt database. Coverage and GC content were calculated using SAMtools, and circular genome visualization was performed with Circos v0.69-9 (Krzywinski et al. 2009). The annotated genome sequences were deposited in GenBank under accession numbers PV929714.1 and PV929715.1.

Codon usage analysis

Coding sequences were extracted from annotated genomes, and codon usage plus Relative Synonymous Codon Usage (RSCU) were calculated using MEGA v11.0.13 (Tamura et al. 2021). Visualization was performed in R v4.3.1 (R Core Team 2023) using the ggplot2 package v3.4.4 (Wickham 2016).

Chloroplast SSRs and repetitive sequences

Chloroplast Simple Sequence Repeats (cpSSRs) were identified with MISA-web (Beier et al. 2017) using thresholds of ≥10 repeats (mono-), ≥5 (di- and tri-), and ≥3 (tetra-, penta-, hexa-nucleotides). Repetitive sequences were detected with REPuter (Kurtz et al. 2001) using a minimum repeat size of 30 bp and a Hamming distance of 3, and classified as forward, reverse, palindromic, or complementary.

Divergent hotspot and phylogenetic analysis

Complete chloroplast genome sequences were aligned in MAFFT v7.520 (Katoh and Standley 2013). Nucleotide diversity (π) was calculated in DnaSP v6.11.01 (Rozas et al. 2017) with a sliding window of 600 bp and a 200 bp step size. Thirteen complete chloroplast genome sequences, including wild-type and mutant *T. flagelliforme*, were aligned in MAFFT v7.520. The best-fit nucleotide substitution model was determined in jModelTest v2.1.10 (Darriba et al. 2012), identifying GTR+G+I as optimal.

Phylogenetic trees were constructed using the Maximum Likelihood method in MEGA v11.0.13 with 1000 bootstrap replicates (Abdullah et al. 2021; Gao et al. 2025).

RESULTS AND DISCUSSION

Chloroplast genome characteristics

The complete chloroplast genomes of wild-type and mutant *Typhonium flagelliforme* were successfully assembled, with lengths of 167,195 bp and 167,204 bp, respectively (Figure 1). Genes on the inside of each circle are transcribed clockwise, while those on the outside are transcribed counterclockwise. Functional gene categories are color-coded, as indicated in the legend. The innermost, darker gray circle represents the GC content. Structural and positional comparisons highlight variations between the wild-type and mutant chloroplast genomes.

Quality assessments confirmed high coverage and uniform GC distribution, ensuring reliability for downstream analyses (Figure 2). From outer to inner rings: contig representation (black), sequencing depth (green for depth >50; red for depth <50), and GC content (purple for GC>50%; brown for GC<50%). The visualization indicates overall high sequence quality and uniform coverage across both genomes, with minor localized variation in depth and GC content. Both exhibited the typical quadripartite structure, LSC, SSC, and two IRs with only minor length variations between genomes. GC content was identical at 36.12%, the highest in IRs and the lowest in SSCs (Table 1). Gene annotation revealed 118 genes in the wild-type and 116 in the mutant, including 73 and 71 protein-coding genes, respectively. Although the mutant genome was 9 bp longer than the wild-type, the GC content remained identical (36.12%), because the length difference was negligible relative to the ~167 kb plastome, and base composition proportions were unchanged; any difference would only appear beyond the reported two-decimal precision. A total of 118 genes were annotated in the wild-type chloroplast genome, whereas the mutant genome contained 116 genes. Several genes were duplicated within the IR regions, including 4 *rRNA* genes (*16S rRNA, 23S rRNA, 5S rRNA, 4.5S rRNA*), 7 *tRNA* genes (*trnA-UGC, trnI-CAU, trnI-GAU, trnL-CAA, trnN-GUU, trnR-ACG, trnV-GAC*), and 8 protein-coding genes (*rpl2, rpl23, rps7, rps12, psbM, ndhB, ycf1, ycf2*) (Table 2). Additionally, 9 protein-coding genes (*rpl2, rpl16, rps16, rpoC1, atpF, ndhA, ndhB, petB, petD*) and 6 *tRNA* genes (*trnA-UGC, trnG-UCC, trnI-GAU, trnL-UAA, trnK-UUU, trnV-UAC*) contained a single intron, while 3 protein-coding genes had two introns (*rps12, clpP, ycf3*) (Table 2). The photosystem-related psaL and petN genes were absent in the mutant, potentially affecting photosynthetic efficiency.

Table 1. Comparative features of the chloroplast genome of wild-type and mutant *Typhonium flagelliforme*

Species	Wild-type	Mutant
Size (bp)	167,195	167,204
LSC (bp)	89,538	89,540
SSC (bp)	14,521	14,521
IRA (bp)	31,567	31,570
IRB (bp)	31,569	31,573
Genes	118	116
CDS	73	71
tRNA	37	37
rRNA	8	8
GC%	36.12	36.12
AT%	63.88	63.88

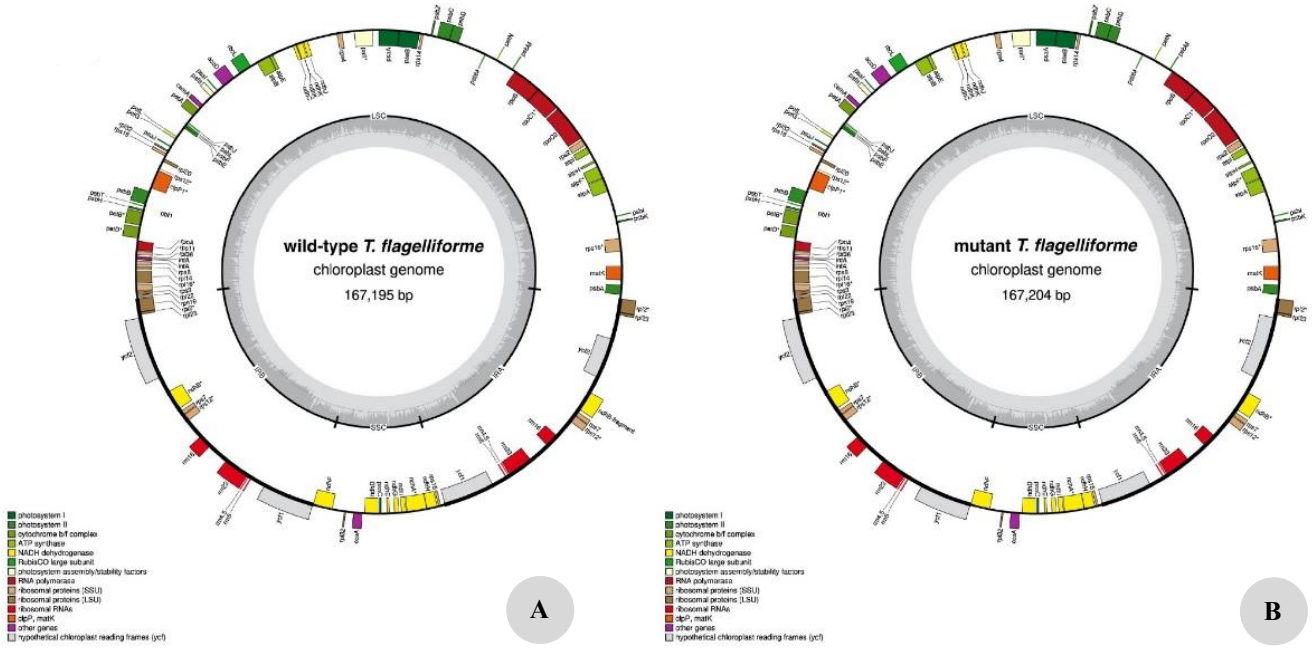

Figure 1. Circular gene map of chloroplast genomes from *Typhonium flagelliforme*: A. Wild-type (167,195 bp), and B. Mutant chloroplast genome (167,204 bp)

Table 2. Comparison of gene content and function between the mutant and wild-type *Typhonium flagelliforme* chloroplast genome

Category	Group of genes	Name of genes in the mutant sample	Name of genes in the wild-type sample
Self-replication	Large subunit of ribosomal proteins	*rpl2a*(2), *rpl14, rpl16a, rpl20, rpl22, rpl23*(2), *rpl32, rpl33, rpl36*	*rpl2a*(2), *rpl14, rpl16a, rpl20, rpl22, rpl23*(2), *rpl32, rpl33, rpl36*
	Small subunit of ribosomal proteins	*rps2, rps3, rps4, rps7*(2), *rps8, rps11, rps12b*(2), *rps14, rps15, rps16a, rps18, rps19*	*rps2, rps3, rps4, rps7*(2), *rps8, rps11, rps12b*(2), *rps14, rps15, rps16a, rps18, rps19*
	DNA-dependent RNA polymerase	*rpoA, rpoB, rpoC1a, rpoC2*	*rpoA, rpoB, rpoC1a, rpoC2*
	Ribosomal RNA genes	*16S rRNA*(2), *23S rRNA*(2), *5S rRNA*(2), *4.5S rRNA*(2)	*16S rRNA*(2), *23S rRNA*(2), *5S rRNA*(2), *4.5S rRNA*(2)
	Transfer RNA genes	*trnA-UGCa*(2), *trnC-GCA, tRNF-GAA, trnG-GCC, trnG-UCCa, trnI-CAU*(2), *trnI-GAUa*(2), *trnL-CAA*(2), *trnL-UAAa, trnL-UAG, trnM-CAU, trnN-GUU*(2), *trnR-ACG*(2), *trnR-UCU, trnS-GGA, trnT-GGU, trnV-GAC*(2), *trnD-GUC, trnE-UUC, trnH-GUG, trnK-UUUa, trnP-UGG, trnQ-UUG, trnS-GCU, trnS-UGA, trnT-UGU, trnV-UACa, trnW-CCA, trnY-GUA, trnfM-CAU*	*trnA-UGCa*(2), *trnC-GCA, tRNF-GAA, trnG-GCC, trnG-UCCa, trnI-CAU*(2), *trnI-GAUa*(2), *trnL-CAA*(2), *trnL-UAAa, trnL-UAG, trnM-CAU, trnN-GUU*(2), *trnR-ACG*(2), *trnR-UCU, trnS-GGA, trnT-GGU, trnV-GAC*(2), *trnD-GUC, trnE-UUC, trnH-GUG, trnK-UUUa, trnP-UGG, trnQ-UUG, trnS-GCU, trnS-UGA, trnT-UGU, trnV-UACa, trnW-CCA, trnY-GUA, trnfM-CAU*
Genes for photosynthesis	Photosystem I	*psaA, psaB, psaC, psaJ*	*psaA, psaB, psaC, psaJ, psaL*
	Photosystem II	*psbA, psbB, psbC, psbD, psbE, psbF, psbH, psbI, psbJ, psbK, psbL, psbM*(2), *psbN (pbf1), psbT, psbZ*	*psbA, psbB, psbC, psbD, psbE, psbF, psbH, psbI, psbJ, psbK, psbL, psbM*(2), *psbN (pbf1), psbT, psbZ*
	RUBISCO	*rbcL*	*rbcL*
	Subunits of ATPsynthase	*atpA, atpB, atpE, atpFa, atpH, atpI*	*atpA, atpB, atpE, atpFa, atpH, atpI*
	Cytochrome b/f complex	*petA, petBa, petDa, petG, petL*	*petA, petBa, petDa, petG, petL, petN*
Other genes	Protease	*clpPb*	*clpPb*
	Maturase	*matK*	*matK*
	Envelope membrane protein	*cemA*	*cemA*
	Translation initiation factor	*infA*	*infA*
	C-type cytochrome synthesis gene	*ccsA*	*ccsA*
	Subunit of Acetyl-CoA-carboxylase	*accD*	*accD*
Genes of unknown function	Conserved hypothetical chloroplast	*ycf1*(2), *ycf2*(2), *ycf3b (pafI), ycf4 (pafII)*	*ycf1*(2), *ycf2*(2), *ycf3b (pafI), ycf4 (pafII)*

Note: (2) indicates the number of the repeat unit is 2, a indicates one intron containing genes, b indicates two intron-containing genes

Codon usage frequency and amino acid composition

A total of 28,274 codons were identified in the complete chloroplast genome of wild-type *T. flagelliforme* and 29,079 codons in the mutant line (Figure 3). The data show a strong codon usage bias, particularly favoring codons ending with A or T, which is typical for chloroplast genomes. Comparative analysis between wild-type and mutant forms reveals slight variations in codon preference that may reflect underlying genomic changes associated with the mutation. In both genomes, the most frequently used codon was UUU (phenylalanine), accounting for 4.16% of all codons in the wild-type and 4.16% in the mutant. The second-most abundant codon was AAA (lysine), with proportions of 4.15% and 4.16%, respectively. By contrast, CGC (Arginine) was the least represented codon in both genomes (0.38% in the wild-type; 0.37% in the mutant). Relative Synonymous Codon Usage (RSCU) analysis revealed a pronounced bias toward codons ending in A or U. In the wild-type genome, 30 codons displayed strong bias (RSCU>1), whereas 29 codons were weakly preferred (RSCU<1); the mutant showed a similar pattern with 31 and 28 codons, respectively. Two codons—AUG (methionine) and UGG (tryptophan)—exhibited no bias (RSCU ≈ 1) in either genome. None of the codons tested (UUU, AAA, CGC) show statistically significant differences in Relative Synonymous Codon Usage (RSCU) between wild-type and mutant genomes ($p>0.94$).

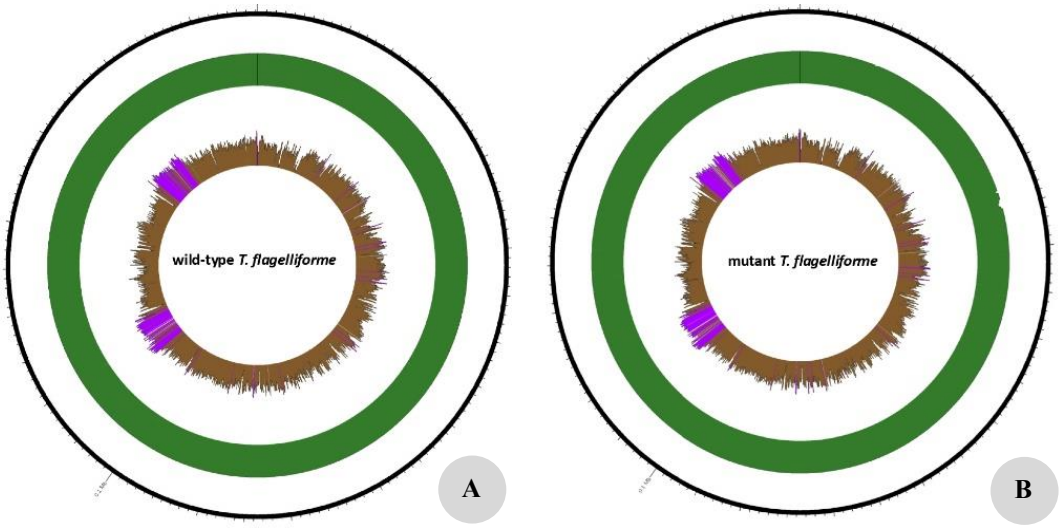

Figure 2. Sequence quality validation of chloroplast genomes from *Typhonium flagelliforme* using circos plots: A. wild-type, and B. mutant

Figure 3. Codon usage frequency distribution in the chloroplast genome of *Typhonium flagelliforme*: A. Wild-type, and B. Mutant. The x-axis represents amino acids and their corresponding codons, while the y-axis indicates the proportion (%) of each codon used for encoding a particular amino acid

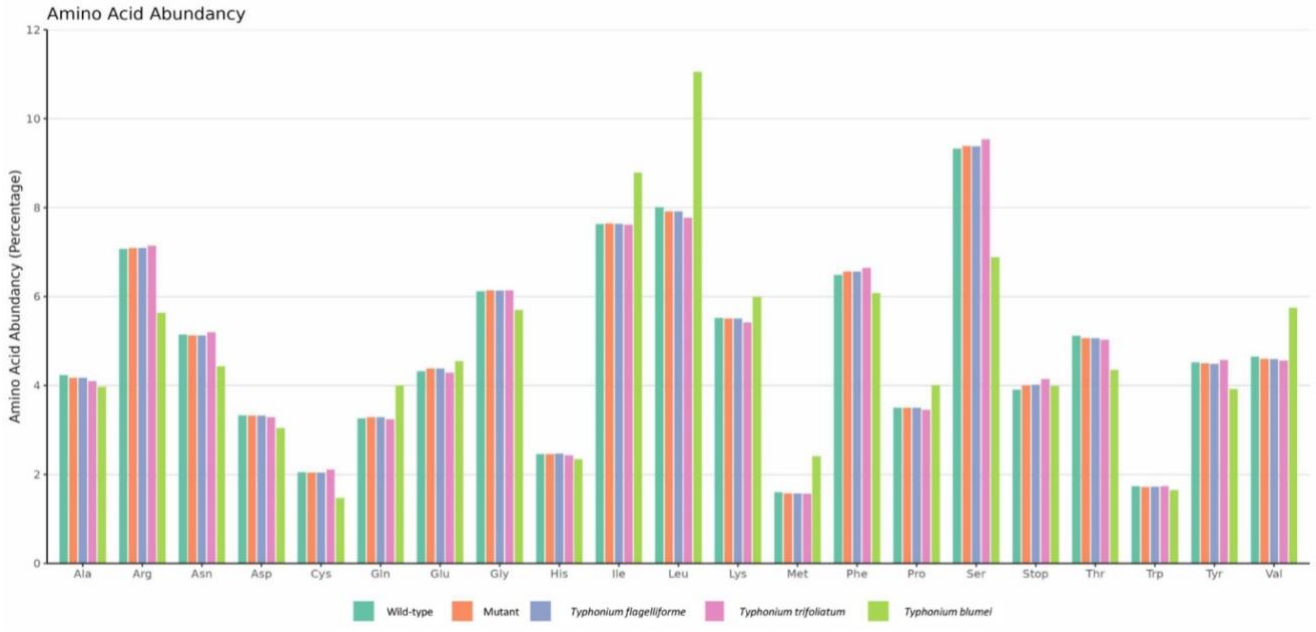

Figure 4. Relative amino acid abundance in the chloroplast genomes of various *Typhonium* species. The bar chart displays the percentage of each amino acid encoded across five samples: wild-type, mutant *Typhonium flagelliforme*, *Typhonium blumei*, and *Typhonium trifoliatum*. The x-axis represents individual amino acids, while the y-axis indicates their relative abundance as a percentage of the total amino acid content

The distribution of amino acids mirrored the codon preferences (Figure 4). The results reveal conserved patterns of amino acid usage across species, with notable variations in residues such as Leucine, Serine, and Proline, suggesting potential links to codon usage bias and chloroplast gene expression dynamics. Phenylalanine was the most abundant amino acid, representing 9.3% of total residues in the wild-type and 9.4% in the mutant. Leucine (8.0% and 7.9%) and isoleucine (7.5%) followed in frequency. The least represented amino acid was methionine, comprising only 1.5% (wild-type) and 1.4% (mutant) of the total. Overall, the amino-acid composition and codon-use profiles of the mutant closely resemble those of the wild-type, indicating that the observed genomic alterations have minimal impact on translational preferences within the chloroplast genome. In addition to coding sequence preferences, examining repetitive elements, such as Simple Sequence Repeats (SSRs) provides valuable information about plastome stability and potential mutational events in the mutant line.

Repetitive sequence and divergent hotspot analysis

Both genomes were rich in A/T mononucleotide SSRs, a common feature in plant plastomes. The wild-type harbored 131 SSRs and the mutant 132 SSRs, with nearly identical motif distributions. In the chloroplast genome of wild-type *T. flagelliforme*, a total of 131 SSRs were identified, including 88 mononucleotides, 18 dinucleotides, 2 trinucleotides, 19 tetranucleotides, and 4 pentanucleotides (Figures 5.A, 5.B). The predominance of A/T mononucleotide repeats is consistent with the AT-rich nature of plant plastomes. The elevated occurrence and diversity of repetitive elements in the mutant genome suggest potential post-mutation structural variations, which could serve as valuable targets for polymorphism-based molecular marker development, comparative plastome analysis, and studies on chloroplast genome evolution in *Typhonium* and related taxa. The most prevalent SSR motif was the A/T mononucleotide repeats (86 occurrences), followed by the AT/AT dinucleotide motif (17 occurrences). SSRs were widely distributed across different regions of the wild-type chloroplast genome, with the majority located in the palindromic repeats (31.6%), followed by forward repeats (29.1%), reverse repeats (20.9%) and complementary repeats (18.4%) (Figure 5.C). SSRs occurred mainly in palindromic and forward repeats, indicating structural stability despite mutation. Sliding window analysis across *T. flagelliforme* variants and related *Typhonium* species identified highly variable loci, particularly *ndhE* and *ccsA,* with the highest nucleotide diversity ($\pi \approx 0.196$ and 0.191, respectively). The co-occurrence of SSRs in or near variable coding regions suggests potential mutational hotspots. These loci represent strong candidates for species-level phylogenetic markers and for tracking plastome evolution under induced mutation.

In comparison, the mutant *T. flagelliforme* chloroplast genome contained 132 SSRs, consisting of 88 mononucleotides, 18 dinucleotides, 2 trinucleotides, 20 tetranucleotides, and 4 pentanucleotides (Figures 6.A, 6.B). The most prevalent SSR motif was the A/T mononucleotide (86 occurrences), followed by the AT/AT dinucleotide motif (17 occurrences). The predominance of A/T-rich mononucleotide SSRs reflects a common feature of plant plastomes, while the relatively higher total SSR count in the mutant compared to the wild-type may indicate structural variation induced by mutation. These SSR-rich and repeat-dense genomic regions represent valuable targets for developing polymorphism-based molecular markers, enabling comparative genomic analyses and evolutionary studies within *Typhonium* and related Araceae taxa. SSRs were

widely distributed across different regions of the mutant chloroplast genome, with the majority located in the palindromic repeats (30.4%), followed by forward repeats (29.8%), reverse repeats (21.5%) and complementary repeats (18.3%) (Figure 6.C). These SSR distributions suggest that mononucleotide A/T-rich regions dominate the repetitive landscape in both chloroplast genomes, which is a common feature of plant chloroplast genomes. Overall, the mutant has a slightly higher number of SSRs, which may indicate post-mutation structural variation. While repeat elements reveal structural characteristics, the identification of divergent hotspot regions facilitates the detection of highly variable loci important for molecular marker development and comparative analysis. Therefore, the co-occurrence of SSRs and divergent hotspots strengthens their value as combined targets for developing polymorphism-based molecular markers and for investigating plastome evolution resulting from induced mutation in the mutant line (Figure 7). Peaks correspond to highly variable genomic regions, with the most divergent loci annotated. These regions are potential candidates for molecular marker development, phylogenetic resolution, and functional studies. The analysis reveals substantial sequence variation not only between the wild-type and mutant *T. flagelliforme,* but also among other *Typhonium* species, providing insight into evolutionary divergence within the genus.

Phylogenetic analysis

Phylogenetic analysis of 13 chloroplast genomes positioned *Typhonium flagelliforme* from the wild-type (PV929714.1) and mutant (PV929715.1) in a well-supported monophyletic group, closely allied to *T. blumei* (MT872311.1, NC_051872.1), while *T. trifoliatum* (MW451769.1) was more distantly related within the genus. Other Araceae genera (*Pinellia ternata* (MT193722.1, ON462056.1, PQ644294.1), *Dieffenbachia seguine* (NC_027272.1), *Arisaema prazeri* (NC_072165.1), *Arisaema nepenthoides* (MW338731.1)) formed separate clades, with *Arabidopsis thaliana* (NC_000932.1) as an outgroup (Figure 8). Bootstrap values (out of 100) are shown at each node and represent the proportion of replicate trees in which the associated taxa clustered together, with higher values indicating stronger branch support. Branch lengths are measured in substitutions per site, reflecting the amount of evolutionary change along each branch, as indicated by the scale bar (0.02). The close clustering of the wild-type and mutant accessions confirms their shared evolutionary lineage, while branch length variation highlights genetic divergence within the *Typhonium* clade. This topology mirrors divergence patterns observed in the hotspot analysis, reinforcing the utility of *ndhE*, *ccsA*, and associated SSRs as phylogenetically informative regions for *Typhonium* and related taxa.

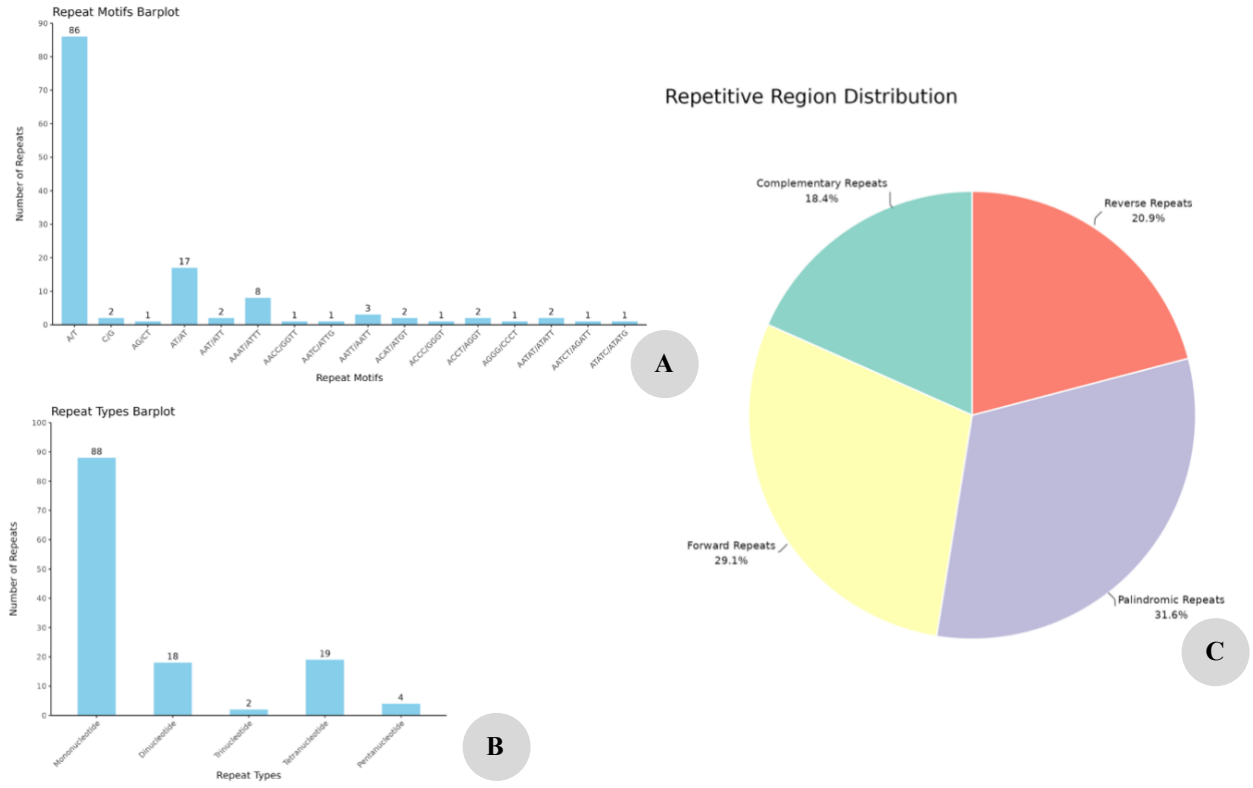

Figure 5. Distribution of Simple Sequence Repeats (SSRs) and repetitive elements in the chloroplast genome of *Typhonium flagelliforme*: A. Frequency of SSR motifs, showing mononucleotide repeats primarily A/T-rich as the most abundant type (86 occurrences), followed by AT/AT dinucleotide motifs (17 occurrences). Tri-, tetra-, and pentanucleotide repeats occur at much lower frequencies, B. Classification of SSR types, with palindromic repeats (31.6%) being the most common, followed by forward repeats (29.8%), reverse repeats (20.3%), and complementary repeats (18.4%), C. Pie chart illustrating the proportional distribution of repetitive sequence types

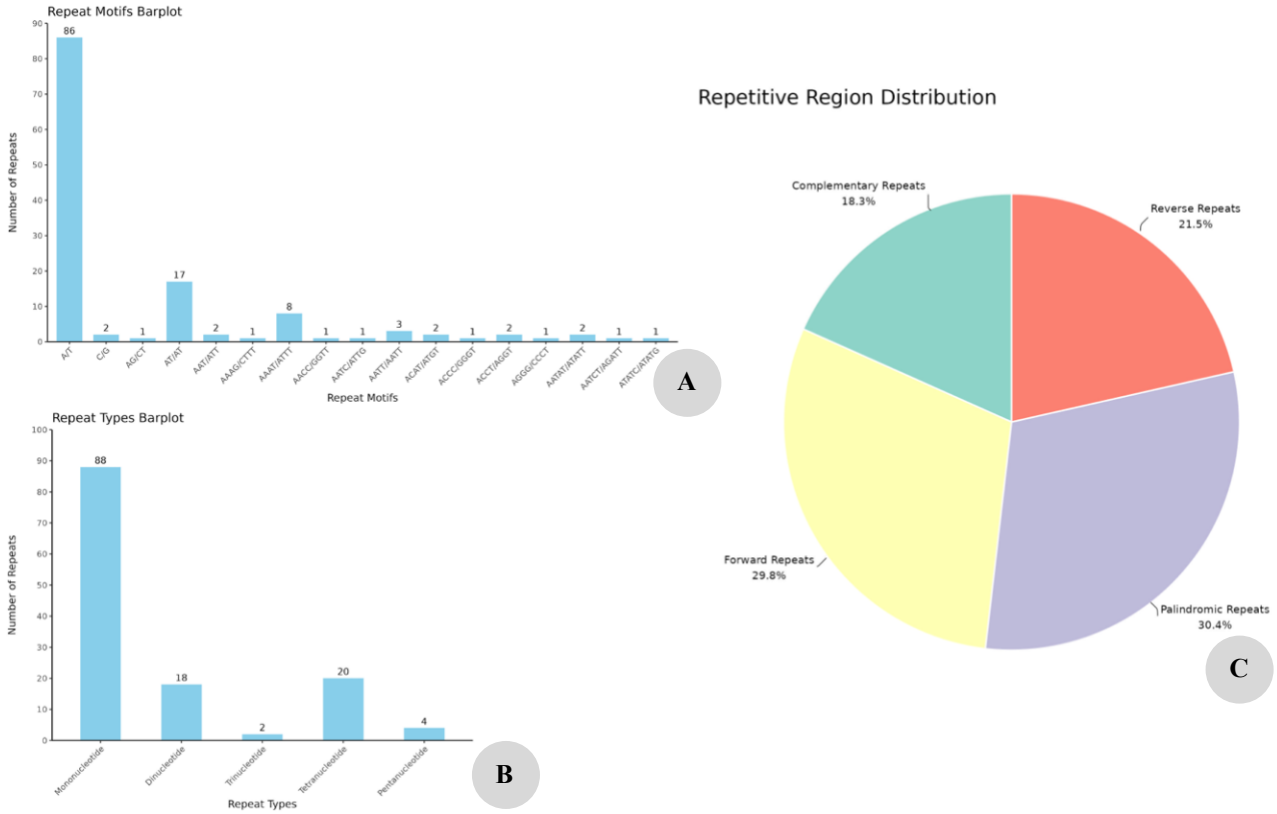

Figure 6. Distribution and classification of Simple Sequence Repeats (SSRs) and repetitive sequences in the chloroplast genome of mutant *Typhonium flagelliforme*: A. Frequency of SSR motifs, showing mononucleotide repeats, particularly A/T-rich motifs, as the most abundant (86 occurrences), followed by dinucleotide repeats (17 occurrences), with lower counts for trinucleotide, tetranucleotide, and pentanucleotide motifs, B. Classification of repeats by type, revealing palindromic repeats as the most frequent (30.4%), followed by forward repeats (29.8%), reverse repeats (21.5%), and complementary repeats (18.3%), C. Proportional distribution of repetitive sequence types across the chloroplast genome

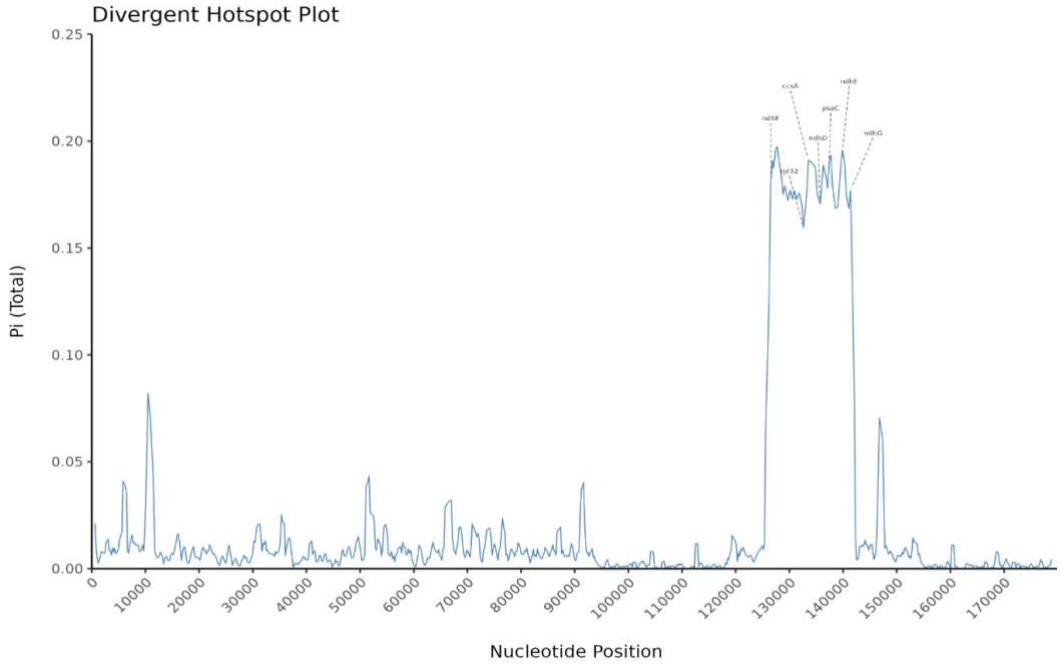

Figure 7. Divergent hotspot plot showing nucleotide diversity (Pi) across the complete chloroplast genomes of *Typhonium* species, including wild-type *Typhonium flagelliforme*, gamma-irradiated mutant *T. flagelliforme*, *Typhonium blumei*, and *Typhonium trifoliatum*. The x-axis represents aligned nucleotide positions along the chloroplast genome, and the y-axis indicates total nucleotide diversity (Pi)

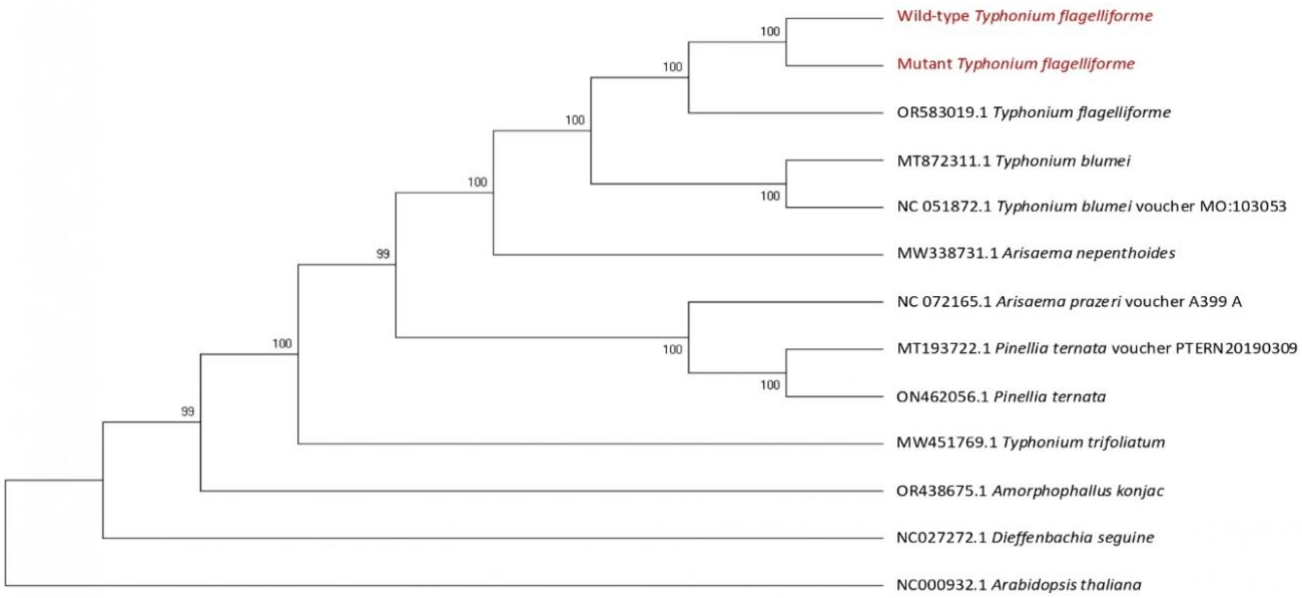

Figure 8. A maximum likelihood phylogenetic tree was reconstructed from complete chloroplast genome sequences of 13 species within the genus *Typhonium* and the family Araceae, using *Arabidopsis thaliana* as the outgroup. The analysis includes wild-type (PV929714.1) and gamma-irradiated mutant *Typhonium flagelliforme* (PV929715.1) from Indonesia

Discussion

High-throughput sequencing has accelerated research on chloroplast genomes, providing complete plastome assemblies and revealing structural variation across angiosperms (Li et al. 2022; Hu et al. 2023). The wild-type *T. flagelliforme* plastome sequenced in this study displayed a conserved quadripartite structure typical of Araceae and monocots (Abdullah et al. 2021; Yin and Gao 2023; Li et al. 2024). Interestingly, the mutant plastome was slightly larger (+9 bp), but exhibited gene losses, specifically *psaL* and *petN*. Such deletions are not uncommon, as structural changes including insertions and rearrangements frequently occur in plant plastomes (Cauz-Santos et al. 2020; Qin et al. 2025). The absence of *psaL*, a subunit of photosystem I crucial for state transitions, and *petN*, a cytochrome b6f component linking PSI and PSII, likely reflects mutagenesis effects of somaclonal variation and gamma irradiation (Sianipar et al. 2016). Despite their functional importance, mutants often maintain or even improve phenotypic performance compared to wild type (Matsuo et al. 2005; Daniell et al. 2016). These findings highlight plastome plasticity, suggesting that *T. flagelliforme* can tolerate gene loss while maintaining metabolic and physiological competence. Additionally, several genes were duplicated in the IR regions, and intron-containing genes followed common chloroplast patterns, with *rps12* identified as a trans-splicing gene, consistent with other Araceae plastomes (Abdullah et al. 2021; Yin and Gao 2023; Li et al. 2024).

Beyond photosynthesis, chloroplasts contribute to pathways generating terpenoids, flavonoids, alkaloids, and phenolic compounds, all central to the medicinal activity of *T. flagelliforme*. Prior studies reported anticancer lectins, antioxidant alkaloids and flavonoids, and apoptosis-modulating terpenoids in this species. The ability of mutant plastomes to sustain or enhance such biosynthesis despite gene loss may reflect adaptive reprogramming of metabolism. Structural variation in plastomes can therefore be harnessed as a molecular tool for metabolic engineering, supporting the development of high-yield phytopharmaceutical lines. The link between plastome evolution and metabolite production underscores the dual ecological and medicinal importance of *T. flagelliforme*.

Genome assembly quality was validated by high sequencing depth and consistent GC content, indicating reliable results (Moss et al. 2020; Chu et al. 2024). Codon usage bias, which influences gene expression and protein folding, was broadly conserved between wild-type and mutant genomes, with a strong preference for A/U-ending codons. The most frequent codons were UUU (phenylalanine) and AAA (lysine), while CGC (arginine) was least represented, consistent with other plastomes, such as *Cocos nucifera* (Aljohi et al. 2016) and *Cycas taitungensis* (Chen et al. 2011). Minor differences in codon counts and Relative Synonymous Codon Usage (RSCU) in the mutant may influence translational kinetics and protein stability (Kimball and Jefferson 2006). Given the role of chloroplasts in supplying precursors for bioactive metabolites, these subtle shifts may indirectly impact metabolic pathways, reinforcing the functional relevance of codon usage patterns.

Repetitive sequence analysis revealed A/T-rich mononucleotide SSRs as the most abundant motifs, consistent with the AT-rich plastomes of higher plants (Qin et al. 2025). While overall patterns were similar, the mutant plastome harbored slightly more tetranucleotide repeats than the wild type, possibly reflecting replication slippage or post-mutagenesis instability (Kim et al. 2006). SSRs are valuable markers for species authentication, germplasm identity, and intra-specific diversity assessment. The

combined use of SSR profiles and divergence hotspots strengthens their application in distinguishing wild-type from mutant lines, particularly for breeding programs and germplasm conservation.

Regions exhibiting high nucleotide diversity (π) were primarily found in single-copy regions, *ndhE*, *ccsA*, *ndhF*, *rpl32*, *ndhD*, *psaC*, and *ndhG*. Among these, *ndhE* and *ccsA* showed the greatest variability, aligning with divergence patterns observed in other Araceae (Xue et al. 2019; Li et al. 2022). These regions represent strong candidates for molecular marker development, supporting phylogenetic resolution, accession identification, and breeding applications, as shown in *Berberis* (Li et al. 2025) and *Paphiopedilum* (Guo et al. 2021). Phylogenetic reconstruction placed wild-type and mutant *T. flagelliforme* in a monophyletic clade closely allied to *T. blumei*, while *T. trifoliatum* appeared more distantly related. Other genera, such as *Pinellia, Arisaema*, and *Dieffenbachia*, formed distinct clades, consistent with earlier Araceae phylogenies (Keating 2004; Nauheimer et al. 2012). This confirms both the genomic stability of *T. flagelliforme* lineages and the taxonomic robustness of the genus.

The genomic insights gained here extend beyond evolutionary inference. Codon usage and SSR profiles can support the authentication of *T. flagelliforme* germplasm, reducing misidentification risks in conservation and cultivation. Divergence hotspots such as *ndhE* and *ccsA* provide reliable markers to distinguish wild-type from mutant accessions, valuable for ex situ strategies aimed at preserving genetic diversity. These genomic tools also have direct applications in in situ conservation by identifying populations that represent unique genetic resources. For breeding programs, hotspot loci can be prioritized in marker-assisted selection, while conservation strategies may integrate cpDNA data to optimize propagation and safeguard genetic integrity.

In conclusion, this study presents a comparative analysis of complete chloroplast genomes from Indonesian wild-type and gamma-irridiated mutant *T. flagelliforme*. Gamma irradiation induces localized plastome alterations in *T. flagelliforme* without disrupting overall genome stability. The discovery of gene losses, codon usage patterns, SSR variation, and divergence hotspots highlights distinct mutational effects while reinforcing conserved chloroplast architecture. These comparative insights provide foundation for both conservation and breeding applications. Integrating these plastome data with nuclear genome analyses in the future will help clarify compensatory mechanisms and strengthen the genomic basis for medicinal plant improvement.

ACKNOWLEDGEMENTS

The authors would like to thank Universitas Bina Nusantara, Indonesia, for the full support provided throughout the course of this study. This research was funded by Universitas Bina Nusantara, grant number 010/ Proyek.Inisiatif/I/2025 awarded to the Food Biotechnology Research Center, Universitas Bina Nusantara.

REFERENCES

Abdullah, Henriquez CL, Mehmood F, Hayat A, Sammad A, Waseem S, Waheed MT, Matthews PJ, Croat TB, Poczai P, Ahmed I. 2021. Chloroplast genome evolution in the *Dracunculus* clade (Aroideae, Araceae). Genomics 113: 183-192. DOI: 10.1016/j.ygeno.2020.12.016.

Aljohi HA, Liu W, Lin Q, Zhao Y, Zeng J, Alamer A, Alanazi IO, Alawad AO, Al-Sadi AM, Hu S, Yu J. 2016. Complete sequence and analysis of coconut palm (*Cocos nucifera*) mitochondrial genome. PLoS One 11 (10): e0163990. DOI: 10.1371/journal.pone.0163990.

Beier S, Thiel T, Münch T, Scholz U, Mascher M. 2017. MISA-web: A web server for microsatellite prediction. Bioinformatics 33 (16): 2583-2585. DOI: 10.1093/bioinformatics/btx198.

Cackett L, Luginbuehl LH, Schreier TB, Lopez-Juez E, Hibberd JM. 2022. Chloroplast development in green plant tissues: The interplay between light, hormone, and transcriptional regulation. New Phytol 233 (5): 2000-2016. DOI: 10.1111/nph.17839.

Cauz-Santos LA, da Costa ZP, Callot C, Cauet S, Zucchi MI, Bergès H, van den Berg C, Vieira MLC. 2020. A repertory of rearrangements and the loss of an inverted repeat region in *Passiflora* chloroplast genomes. Genome Biol Evol 12: 1841-1857. DOI: 10.1093/gbe/evaa155.

Chen H, Deng L, Jiang Y, Lu P, Yu J. 2011. RNA editing sites exist in protein-coding genes in the chloroplast genome of *Cycas taitungensis*. J Integr Plant Biol 53 (12): 961-970. DOI: 10.1111/j.1744-7909.2011.01082.x.

Chu L, Du Q, Zuo S, Liu G, Wang H, Liu G, Zhao L, Xu G. 2024. Assembly and comparative analysis of the complete mitochondrial genome of *Vaccinium carlesii* Dunn. Genomics 116 (5): 110897. DOI: 10.1016/j.ygeno.2024.110897.

Danecek P, Bonfield JK, Liddle J, Marshall J, Ohan V, Pollard MO, Whitwham A, Keane T, McCarthy SA, Davies RM, Li H. 2021. Twelve years of SAMtools and BCFtools. GigaScience 10 (2): giab008. DOI: 10.1093/gigascience/giab008.

Daniell H, Lin C-S, Yu M, Chang W-J. 2016. Chloroplast genomes: Diversity, evolution, and applications in genetic engineering. Genome Biol 17 (1): 134. DOI: 10.1186/s13059-016-1004-2.

Darriba D, Taboada GL, Doallo R, Posada D. 2012. jModelTest 2: More models, new heuristics and parallel computing. Nat Methods 9 (8): 772. DOI: 10.1038/nmeth.2109.

De Coster W, D'Hert S, Schultz DT, Cruts M, Van Broeckhoven C. 2018. NanoPack: Visualizing and processing long-read sequencing data. Bioinformatics 34: 2666-2669. DOI: 10.1093/bioinformatics/bty149.

Gao Z, Cai Y, Long J, Wang B, Huang Z, Gao Y. 2025. The complete chloroplast genome and the phylogenetic analysis of *Fimbristylis littoralis* (Cyperaceae) collected in cherry blossom nursery. Intl J Mol Sci 26 (5): 2321. DOI: 10.3390/ijms26052321.

Greiner S, Lehwark P, Bock R. 2019. OrganellarGenomeDRAW (OGDRAW) Version 1.3.1: Expanded toolkit for the graphical visualization of organellar genomes. Nucleic Acids Res 47 (W1): W59-W64. DOI: 10.1093/nar/gkz238.

Guo Y-Y, Yang J-X, Bai M-Z, Zhang G-Q, Liu Z-J. 2021. The chloroplast genome evolution of Venus slipper (*Paphiopedilum*): IR expansion, SSC contraction, and highly rearranged SSC regions. BMC Plant Biol 21 (1): 248. DOI: 10.1186/s12870-021-03053-y.

Gurevich A, Saveliev V, Vyahhi N, Tesler G. 2013. QUAST: Quality Assessment Tool for genome assemblies. Bioinformatics 29 (8): 1072-1075. DOI: 10.1093/bioinformatics/btt086.

Hu Y, Sun Y, Zhu Q-H, Fan L, Li J. 2023. Poaceae chloroplast genome sequencing: Great leap forward in recent ten years. Curr Genomics 23 (6): 369-384. DOI: 10.2174/1389202924666221201140603.

Jeong GH, Kaur S, Yoo Y, Ryu YB, Lee SJ, Jung K-W, Chung M-S, Bai H-W, Kim J-H, Lee S, Kim TH, Chung BY, Lee SS. 2024. Effects of gamma irradiation on changes in chemical composition and antioxidant activity of *Euphorbia maculata* callus. Plants 13 (16): 2306. DOI: 10.3390/plants13162306.

Katoh K, Standley DM. 2013. MAFFT multiple sequence alignment software version 7: Improvements in performance and usability. Mol Biol Evol 30 (4): 772-780. DOI: 10.1093/molbev/mst010.

Keating R. 2004. Vegetative anatomical data and its relationship to a revised classification of the genera of Araceae. Ann Missouri Bot Gard 91 (3): 485-494.

Kim YS, Schumaker KS, Zhu J-K. 2006. EMS mutagenesis of *Arabidopsis*. Methods Mol Biol 323: 101-103. DOI: 10.1385/1-59745-003-0:101.

Kimball SR, Jefferson LS. 2006. New functions for amino acids: Effects on gene transcription and translation. Am J Clin Nutr 83 (2): 500S-507S. DOI: 10.1093/ajcn/83.2.500s.

Kolmogorov M, Yuan J, Lin Y, Pevzner PA. 2019. Assembly of long, error-prone reads using repeat graphs. Nat Biotechnol 37 (5): 540-546. DOI: 10.1038/s41587-019-0072-8.

Krzywinski M, Schein J, Birol I, Connors J, Gascoyne R, Horsman D, Jones SJ, Marra MA. 2009. Circos: An information aesthetic for comparative genomics. Genome Res 19 (9): 1639-1645. DOI: 10.1101/gr.092759.109.

Kurtz S, Choudhuri JV, Ohlebusch E, Schleiermacher C, Stoye J, Giegerich R. 2001. REPuter: The manifold applications of repeat analysis on a genomic scale. Nucleic Acids Res 29 (22): 4633-4642. DOI: 10.1093/nar/29.22.4633.

Lai C-S, Mas RHMH, Nair NK, Majid MIA, Mansor SM, Navaratnam V. 2008. *Typhonium flagelliforme* inhibits cancer cell growth in vitro and induces apoptosis: An evaluation by the bioactivity guided approach. J Ethnopharmacol 118 (1): 14-20. DOI: 10.1016/j.jep.2008.02.034.

Li B, Liu T, Ali A, Xiao Y, Shan N, Sun J, Huang Y, Zhou Q, Zhu Q. 2022. Complete chloroplast genome sequences of three aroideae species (Araceae): Lights into selective pressure, marker development and phylogenetic relationships. BMC Genomics 23 (1): 218. DOI: 10.1186/s12864-022-08400-3.

Li H, Abdullah, Yang H, Guo H, Yuan Y, Ahmed I, Li G, Wang Y, Chang Y, Tian X. 2025. Chloroplast genome evolution of *Berberis* (Berberidaceae): Implications for phylogeny and metabarcoding. Gene 933: 148959. DOI: 10.1016/j.gene.2024.148959.

Li H. 2018. Minimap2: Pairwise alignment for nucleotide sequences. Bioinformatics 34: 3094-3100. DOI: 10.1093/bioinformatics/bty191.

Li L, Yang M, Qi Y, Yu Y, Gao P, Yang S, Zhao Y, Guo J, Liu J, Huang F, Yu L. 2024. Complete chloroplast genome and phylogenetic analysis of *Amorphophallus paeoniifolius* (Araceae). Mitochondrial DNA B Resour 9: 865-870. DOI: 10.1080/23802359.2024.2378966.

Matsuo M, Ito Y, Yamauchi R, Obokata J. 2005. The rice nuclear genome continuously integrates, shuffles, and eliminates the chloroplast genome to cause chloroplast-nuclear DNA flux. Plant Cell 17 (3): 665-675. DOI: 10.1105/tpc.104.027706.

Mohan S, Abdul AB, Abdelwahab SI, Al-Zubairi AS, Sukari MA, Abdullah R, Taha MME, Beng NK, Isa NM. 2010. *Typhonium flagelliforme* inhibits the proliferation of murine leukemia WEHI-3 cells in vitro and induces apoptosis in vivo. Leuk Res 34 (11): 1483-1492. DOI: 10.1016/j.leukres.2010.04.023.

Moss EL, Maghini DG, Bhatt AS. 2020. Complete, closed bacterial genomes from microbiomes using nanopore sequencing. Nat Biotechnol 38 (6): 701-707. DOI: 10.1038/s41587-020-0422-6.

Nauheimer L, Metzler D, Renner SS. 2012. Global history of the ancient monocot family Araceae inferred with models accounting for past continental positions and previous ranges based on fossils. New Phytol 195 (4): 938-950. DOI: 10.1111/j.1469-8137.2012.04220.x.

Nobakht GM, Kadir MA, Stanslas J, Charng CW. 2014. Cytotoxic effect of *Typhonium flagelliforme* extract. J Med Plants Res 8 (31): 1021-1024. DOI: 10.5897/jmpr11.915.

Okonechnikov K, Conesa A, García-Alcalde F. 2016. Qualimap 2: Advanced multi-sample quality control for high-throughput sequencing data. Bioinformatics 32 (2): 292-294. DOI: 10.1093/bioinformatics/btv566.

Purnamaningsih R, Sianipar NF, Assidqi K, Warnars HLHS. 2018. Genetic variation of somaclonal mutants from the 8th generation of Pekalongan accession rodent tuber (*Typhonium flagelliforme* Lodd.) based on RAPD-PCR analysis. IOP Conf Ser: Earth Environ Sci 195: 012054. DOI: 10.1088/1755-1315/195/1/012054.

Qin Q, Dong Y, Chen J, Wang B, Peng Y, Zhang X, Wang X, Zeng J, Zhong G, Zhang S, Du X. 2025. Comparative analysis of chloroplast genomes reveals molecular evolution and phylogenetic relationships within the Papilionoideae of Fabaceae. BMC Plant Biol 25 (1): 157. DOI: 10.1186/s12870-025-06138-0.

R Core Team. 2023. R: A language and environment for statistical computing. R Foundation for Statistical Computing, Vienna (AT). https://www.R-project.org/.

Rozas J, Ferrer-Mata A, Sánchez-DelBarrio JC, Guirao-Rico S, Librado P, Ramos-Onsins SE, Sánchez-Gracia A. 2017. DnaSP 6: DNA sequence polymorphism analysis of large datasets. Mol Biol Evol 34 (12): 3299-3302. DOI: 10.1093/molbev/msx248.

Sianipar NF, Assidqi K, Hadisaputri YE, Salam S, Purnamaningsih R, So IG. 2023. Mutant plant Tipobio variety of rodent tuber (*Typhonium flagelliforme*): Fatty acids compounds and in vitro anticancer activity. E3S Web Conf 388: 01032. DOI: 10.1051/e3sconf/202338801032.

Sianipar NF, Hadisaputri YE, Assidqi K, Salam S, Yusuf M, Destiarani W, Purnamaningsih R, So IG, Takara K, Asikin Y. 2024. In silico and in vitro characterizations of rodent tuber (*Typhonium flagelliforme*) mutant plant isolates against FXR receptor on MCF-7 cells. J Oleo Sci 73 (10): 1349-1360. DOI: 10.5650/jos.ess24020.

Sianipar NF, Purnamaningsih R, Gumanti DL, Rosaria, Vidianty M. 2017. Analysis of gamma irradiated-third generation mutants of rodent tuber (*Typhonium flagelliforme* Lodd.) based on morphology, RAPD, and GC-MS markers. Pertanika J Trop Agric Sci 40 (1): 185-202.

Sianipar NF, Purnamaningsih R, Rosaria. 2016. Bioactive compounds of fourth generation gamma-irradiated *Typhonium flagelliforme* Lodd. mutants based on gas chromatography-mass spectrometry. IOP Conf Ser: Earth Environ Sci 41: 012025. DOI: 10.1088/1755-1315/41/1/012025.

Sianipar NF, Purnamaningsih R. 2018. Enhancement of the contents of anticancer bioactive compounds in mutant clones of rodent tuber (*Typhonium flagelliforme* Lodd.) based on GC-MS analysis. Pertanika J Trop Agric Sci 41 (1): 305-320.

Sianipar NF, Wantho A, Rustikawati, Maarisit W. 2013. The effects of gamma irradiation on growth response of rodent tuber (*Typhonium flagelliforme* Lodd.) mutant in in vitro culture. Hayati J Biosci 20 (2): 51-56. DOI: 10.4308/hjb.20.2.51.

Song J-H, Yang S, Choi G, Park I. 2023. Characterization of the complete chloroplast genome of the important herbal medicinal plant, *Thymus quinquecostatus* (Lamiaceae). J Asia-Pac Biodivers 16 (1): 140-143. DOI: 10.1016/j.japb.2022.12.010.

Tamura K, Stecher G, Kumar S. 2021. MEGA11: Molecular Evolutionary Genetics Analysis version 11. Mol Biol Evol 38 (7): 3022-3027. DOI: 10.1093/molbev/msab120.

Tillich M, Lehwark P, Pellizzer T, Ulbricht-Jones ES, Fischer A, Bock R, Greiner S. 2017. GeSeq-versatile and accurate annotation of organelle genomes. Nucleic Acids Res 45 (W1): W6-W11. DOI: 10.1093/nar/gkx391.

Wang W, Lanfear R. 2019. Long-reads reveal that the chloroplast genome exists in two distinct versions in most plants. Genome Biol Evol 11 (12): 3372-3381. DOI: 10.1093/gbe/evz256.

Wickham H. 2016. Ggplot2: Elegant Graphics for Data Analysis. Springer-Verlag, New York. DOI: 10.1007/978-3-319-24277-4_9.

Xue T, Zhang H, Zhang Y, Wei S, Chao Q, Zhu Y, Teng J, Zhang A, Sheng W, Duan Y, Xue J. 2019. Full-length transcriptome analysis of shade-induced promotion of tuber production in *Pinellia ternata*. BMC Plant Biol 19 (1): 565. DOI: 10.1186/s12870-019-2197-9.

Yan K, Lu X, Li W, Sun C, Zhou X, Wang Y. 2025. Chloroplast genome diversity and molecular evolution in Hypericaceae: New insights from three *Hypericum* species. Intl J Mol Sci 26 (1): 323. DOI: 10.3390/ijms26010323.

Yin S, Gao Y. 2023. The complete chloroplast genome assembly of *Amorphophallus krausei* Engler, Pflanzenr 1911 (Araceae) from southwestern China. Mitochondrial DNA B Resour 8 (12): 1339-1342. DOI: 10.1080/23802359.2023.2288889.

Zhao C, Xu W, Huang Y, Sun Q, Wang B, Chen C, Chen Q. 2021. Chloroplast genome characteristics and phylogenetic analysis of the medicinal plant *Blumea balsamifera* (L.) DC. Genet Mol Biol 44 (4): e20210095. DOI: 10.1590/1678-4685-gmb-2021-0095.